*J Physiol* 589.2 (2011) pp 283–295



The Journal of Physiology

# The dynamics of single spike-evoked adenosine release in the cerebellum

Boris P. Klyuch[1], Magnus J. E. Richardson[2], Nicholas Dale[1] and Mark J. Wall[1]

[1] *Department of Biological Sciences and* [2] *Warwick Systems Biology Centre, University of Warwick, Coventry CV4 7AL, UK*

**Non-technical summary** Adenosine modulates brain activity in both health and disease. Although we know a lot about adenosine action, we know little about how it is released and its cellular sources. We have previously shown that adenosine can be released in the cerebellum by a train of action potentials. Here we have used a pharmacological agent to enhance adenosine release and can thus study release in response to a single action potential. The release follows a waveform that is well described by a minimal diffusion model from a temporally sharp release event. Adenosine release has a complex, history-dependent dynamics: it can be either depressed or enhanced depending on the stimulation pattern – similar properties to those of fast neurotransmitters such as glutamate. Our results demonstrate that the dynamics of adenosine release will depend strongly on the pattern of neural activity and thus constitutes a highly complex signalling pathway in the nervous system.

**Abstract** The purine adenosine is a potent neuromodulator in the brain, with roles in a number of diverse physiological and pathological processes. Modulators such as adenosine are difficult to study as once released they have a diffuse action (which can affect many neurones) and, unlike classical neurotransmitters, have no inotropic receptors. Thus rapid postsynaptic currents (PSCs) mediated by adenosine (equivalent to mPSCs) are not available for study. As a result the mechanisms and properties of adenosine release still remain relatively unclear. We have studied adenosine release evoked by stimulating the parallel fibres in the cerebellum. Using adenosine biosensors combined with deconvolution analysis and mathematical modelling, we have characterised the release dynamics and diffusion of adenosine in unprecedented detail. By partially blocking $K^+$ channels, we were able to release adenosine in response to a single stimulus rather than a train of stimuli. This allowed reliable sub-second release of reproducible quantities of adenosine with stereotypic concentration waveforms that agreed well with predictions of a mathematical model of purine diffusion. We found no evidence for ATP release and thus suggest that adenosine is directly released in response to parallel fibre firing and does not arise from extracellular ATP metabolism. Adenosine release events showed novel short-term dynamics, including facilitated release with paired stimuli at millisecond stimulation intervals but depletion-recovery dynamics with paired stimuli delivered over minute time scales. These results demonstrate rich dynamics for adenosine release that are placed, for the first time, on a quantitative footing and show strong similarity with vesicular exocytosis.

(Received 2 September 2010; accepted after revision 15 November 2010; first published online 15 November 2010)
**Corresponding author** M. J. Wall: Department of Biological Sciences, University of Warwick, Coventry CV4 7AL, UK. Email: mark.wall@warwick.ac.uk

**Abbreviations** EPSP, excitatory postsynaptic potential; PF, parallel fibre; PSC, postsynaptic current; PSP, postsynaptic potential.



DOI: 10.1113/jphysiol.2010.198986

## Introduction

The neuromodulator adenosine is involved in diverse CNS processes including sleep, locomotion and respiration, and provides neuroprotection during hypoxia, epilepsy and ischaemia (Boison, 2006; Dale & Frenguelli, 2009). The actions of adenosine, via a number of G-protein coupled cell-surface receptors, are well characterised (Fredholm *et al*. 2000, 2001) and typically reduce activity within neural networks. However, the mechanism of adenosine release into the extracellular space and the dynamics of its subsequent diffusion to reach and activate these receptors are still unclear in many areas of the brain. Adenosine release can follow extracellular ATP metabolism from ATP released by exocytosis (Edwards *et al*. 1992; Dale, 1998; Jo & Schlicter, 1999) or via gap junction hemi-channels (Pearson *et al*. 2005). Adenosine can also be transported out of the cell cytoplasm by specific transporter proteins (Craig & White, 1993; Sweeney, 1996).

There is growing evidence that neural activity can trigger adenosine release: trains of action potentials release adenosine in the hippocampus (Mitchell *et al*. 1993), calyx of Held (Kimura *et al*. 2003; Wong *et al*. 2006) and cerebellum (Wall & Dale, 2007, 2008). This provides a potentially important negative feedback mechanism to modulate the level of activity within neural networks and also provides a possible link between neural activity and local blood flow (Li & Iadecola, 1994). The exact mechanisms for this adenosine release have not been fully elucidated, but the most detailed study has been carried out in the cerebellum (Wall & Dale, 2007, 2008). Local activation, within the molecular layer releases adenosine by a process that is both action potential and $Ca^{2+}$ dependent and does not appear to involve extracellular ATP metabolism or transporter proteins (Wall & Dale, 2007). Additionally, the modulation of adenosine release by specific G-protein coupled receptor agonists strongly suggests the requirement of parallel fibre activity (Wall & Dale, 2007, 2008).

Unlike the description of the effects of fast synaptic neurotransmitters – the rise and fall of postsynaptic potentials (PSPs) and short-term plasticity (depression and facilitation), the dynamics of neuromodulator release has not been characterised. Here, we use a novel manipulation of the adenosine release mechanism to trigger reliable pulses of neuromodulator release from which the properties and dynamics of release can be studied. We demonstrate that adenosine release shares many characteristics of conventional transmitter release – dependence on action potential width and homosynaptic plasticity.

## Methods

### Preparation of cerebellar slices

Transverse slices of cerebellar vermis (400 $\mu$m) were prepared from male Wistar rats, at postnatal days 21–28. As described previously (Wall & Dale, 2007) and in accordance with the UK Animals (Scientific Procedures) Act 1986, rats were killed by cervical dislocation and then decapitated. The cerebellum was rapidly removed and cerebellar slices were cut on a Microm HM 650V microslicer (Carl Zeiss) in cold (2–4°C) high $Mg^{2+}$, low $Ca^{2+}$ artificial cerebrospinal fluid (aCSF), composed of (mM): 127 NaCl, 1.9 KCl, 8 $MgCl_2$, 0.5 $CaCl_2$, 1.2 $KH_2PO_4$, 26 $NaHCO_3$, 10 D-glucose (pH 7.4 when bubbled with 95% $O_2$ and 5% $CO_2$). Slices were stored in normal ACSF (1.3 mM $MgCl_2$, 2.4 mM $CaCl_2$) at room temperature for 1–6 h before recording.

### Recording from slices

An individual slice was transferred to a recording chamber, submerged in ACSF and perfused at 6 ml $min^{-1}$ (30–32°C). For stimulation (to evoke purine release and excitatory postsynaptic potentials, EPSPs), square voltage pulses (2–5 V, 200 $\mu$s duration) were delivered by an isolated pulse stimulator (ISO-STIM 01M, NPI Electronics, Tamm, Germany) via a concentric bipolar metal stimulating electrode (FHC Inc., Bowdoin, ME, USA) placed on the surface of the molecular layer. Purine biosensors were either positioned just above the surface of the slice (bent so their longitudinal surface was parallel to the stimulated molecular layer) or carefully inserted into the molecular layer. For extracellular recording, an aCSF filled microelectrode was placed on the same track along which the parallel fibres travel. Parallel fibre EPSPs will represent the sum of Purkinje cell, Bergmann glia and molecular layer interneuron EPSPs. Extracellular recordings were made using an EXT-10C extracellular amplifier (NPI Electronics), filtered at 1 kHz and digitised on-line (10 kHz) with a Micro 1401 interface controlled by Spike2 software (v. 6.1) (Cambridge Electronic Design, Cambridge, UK).

### Biosensor characteristics

Biosensors (Llaudet *et al*. 2003, 2005) were obtained from Sarissa Biomedical Ltd (Coventry, UK). Three types of purine biosensor were used in this study. Firstly, a screened null sensor, possessing the matrix but no enzymes, was used to control for the release of any non-specific electro-active interferents. Secondly,

screened ADO biosensors (Llaudet *et al.* 2003) containing adenosine deaminase, nucleoside phosphorylase and xanthine oxidase (responsive to adenosine, inosine and hypoxanthine). Finally, screened ATP biosensors, which consisted of the entrapped enzymes glycerol kinase and glycerol-3-phosphate oxidase (Llaudet *et al.* 2005). Glycerol (2 mM) was included in the aCSF, as a co-substrate required for ATP detection. A full description of the properties of the biosensors has already been published (Llaudet *et al.* 2003, 2005), but they show a linear response to increasing concentration of analyte and are fast to respond. Biosensors were calibrated before the slice was present in the perfusion chamber and after the slice had been removed, allowing measurement of any reduction in sensitivity during the experiment. ADO biosensors detect adenosine, inosine and hypoxanthine. In many experiments, particularly when purines were released by a train of stimuli in 4-AP, the precise composition of the purines released was not defined. Therefore, in order to calculate the concentration of purines detected by ADO biosensors, the adenosine calibration was used to give either $\mu$M′ or nM′ of purines (as outlined in Pearson *et al.* 2001). This was possible as ADO biosensors have an approximately equal sensitivity to adenosine, inosine and hypoxanthine. Biosensor calibration currents were not affected by 4-AP. Biosensor signals were acquired at 1 kHz with a Micro 1401 interface using Spike2 (v. 6.1) software (Cambridge Electronics Design).

### Measuring extracellular ATP breakdown

To measure the extracellular breakdown of ATP, ADO and ATP, biosensors were inserted into different molecular layers within a transverse cerebellar slice. A perfusion pipette (PDES-02DX, NPI Electronics) was used to inject 10 $\mu$M ATP (1 s pulse) into the slice. The perfusion pipette was moved between the molecular layer containing the ATP sensor and the molecular layer containing the ADO sensor such that injections were made at the same distance from each biosensor (between 0.5 and 1 mm). Injection of aCSF produced no current on either biosensor.

### Drugs

All drugs were made up as 10–100 mM stock solutions, stored frozen and then thawed and diluted with aCSF on the day of use. Adenosine, 8-cyclopentyltheophylline (8CPT), 4-aminopyridine (4-AP) and sodium polyoxotungstate (POM-1) were purchased from Sigma-Aldrich (Poole, UK). Erythro-9-(2-hydroxy-3-nonyl)adenine (EHNA), 2,3-dioxo-6-nitro-1,2,3,4-tetrahydrobenzo[f]quinoxaline -7-sulfonamide (NBQX), 4-(8-chloro-2-methyl-11*H*-imidazo[1,2-c][2,3]benzodiazepin-6-benzeneamine dihydrochloride (GYKI 47261) and D-(–)-2-amino-5-phosphonopentanoic acid (D-AP5) were purchased from Tocris-Cookson (Bristol, UK). Kynurenic acid, tetrodotoxin (TTX) and 6- cyano-7-nitroquinoxaline-2,3-dione (CNQX) were purchased from Ascent Scientific (Bristol, UK). ATP was purchased from Roche (Welwyn Garden City, UK).

The data are presented as means ± standard error of the mean (S.E.M.). Statistical analysis was performed using Student's *t* test. The significance level was set at $P < 0.05$.

## Results

Adenosine release can be evoked in the molecular layer of cerebellar slices by trains of action potentials and measured in real-time by an ADO biosensor placed on the slice surface (Wall & Dale, 2007). Several lines of evidence suggest that parallel fibre activity is required for this release and that parallel fibres may themselves directly release adenosine (Wall & Dale, 2007, 2008). We have taken the novel approach of enhancing the probability of adenosine release using the $K^+$ channel blocking drug 4-aminopyridine (4-AP). This has allowed us to measure release of the purine adenosine in response to a single stimulus and thus to investigate its release properties in unprecedented detail.

### 4-AP increases action potential-dependent purine release

Microelectrode biosensors (Llaudet *et al.* 2003) were used to characterise the effects of 4-AP on molecular-layer adenosine release. Application of 4-AP (10–1000 $\mu$M) induced a concentration-dependent increase in the ADO biosensor current following stimulation (40–100 stimuli, 20 Hz, Fig. 1*A* and *B*). This increase was due to purine detection, as there was no current on null sensors ($n = 15$, Fig. 1*A*). As in control (release evoked by 40–100 stimuli at 20 Hz in the absence of 4-AP, Wall & Dale, 2007), purine release in 4-AP was both action potential (blocked by 0.5–1 $\mu$M TTX, $n = 8$) and $Ca^{2+}$ dependent (blocked by zero $Ca^{2+}$ aCSF, $n = 3$). To produce detectable adenosine release, 40–100 stimuli (20 Hz) are normally required (in the absence of 4-AP, Wall & Dale, 2007). However, with increasing concentrations of 4-AP the number of stimuli required could be decreased until a single stimulus was sufficient (this occurred at ∼60 $\mu$M 4-AP, Fig. 1*C*). To investigate whether the purine released in 4-AP is adenosine, the adenosine deaminase inhibitor EHNA was used. EHNA prevents the conversion of adenosine to inosine and prevents ADO biosensors detecting adenosine with no effect on the detection of the

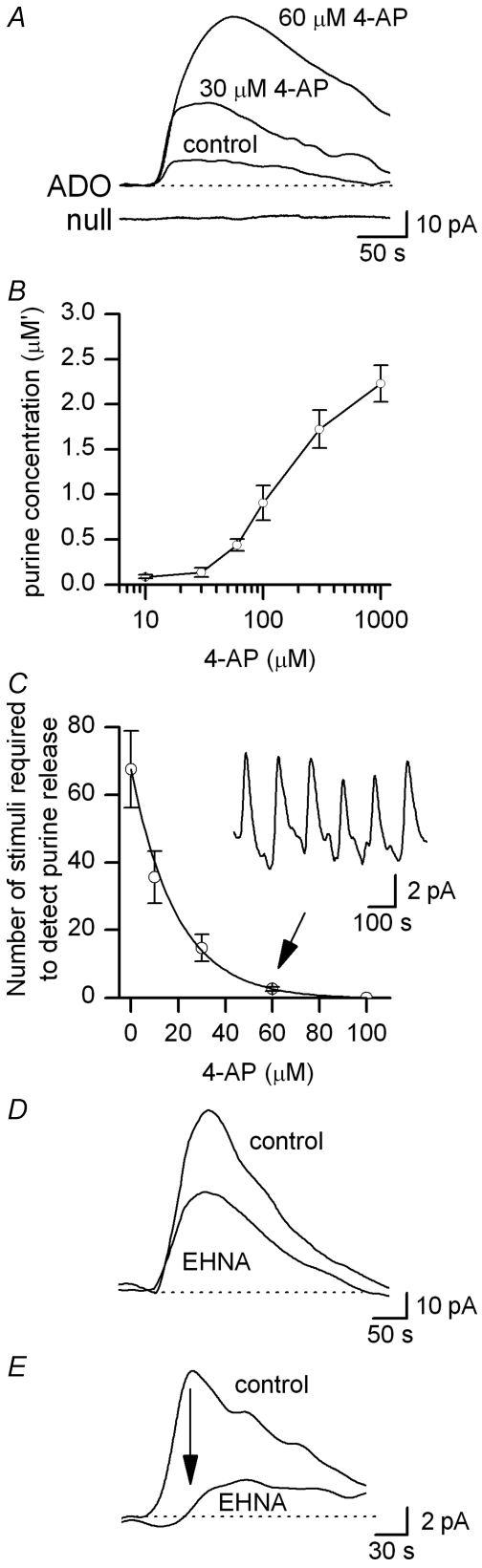


**Figure 1. 4-AP enhances purine release**
*A*, superimposed traces from adenosine (ADO) and null biosensors placed on the surface of the molecular layer in control and in 4-AP (30 $\mu$M and 60 $\mu$M). Purine release (in response to fifty 20 Hz stimuli) was enhanced by 4-AP (no response on closely positioned null sensor). *B*, summary of purine release over a range of 4-AP concentrations ($n = 4$–6). *C*, the mean number of stimuli required to produce detectable purine release (~20 pA current on ADO biosensor) plotted against 4-AP concentration ($n = 5$). At around 60 $\mu$M 4-AP, a single stimulus was sufficient to produce purine release. Above 100 $\mu$M 4-AP, spontaneous purine release occurred (zero stimuli required for release). The data are fitted with a single exponential (time constant = 19.5 $\mu$M). Inset, ADO biosensor trace showing purine release in response to single stimuli (in 60 $\mu$M 4-AP, a single stimulus was given every 300 s). *D*, superimposed traces from an adenosine (ADO) biosensor in control (60 $\mu$M 4-AP) and in 4-AP plus EHNA (20 $\mu$M) following electrical stimulation (60 stimuli, 20 Hz). EHNA reduced the current amplitude by ~40%. *E*, superimposed traces from an ADO biosensor in control (60 $\mu$M 4-AP) and in the presence of 4-AP plus EHNA (20 $\mu$M). Purine release (following a single stimulus) was greatly reduced by EHNA. Thus virtually all the current at the peak (arrow) was produced by adenosine.

adenosine metabolites inosine and hypoxanthine (Wall & Dale, 2007). Following a train of stimuli (in 60 $\mu$M 4-AP), EHNA reduced the current amplitude by 38 ± 3% ($n = 5$ slices, Fig. 1*D*). Thus although a proportion of the purines released in 4-AP is adenosine, the proportion appears less than in control conditions (~75%, Wall & Dale, 2007). This may reflect an inability of the EHNA to prevent the metabolism of large quantities of released adenosine or there may be direct release of the adenosine metabolites inosine and hypoxanthine. In contrast, EHNA (20 $\mu$M) markedly reduced the ADO biosensor current produced by a single stimulus (in 60 $\mu$M 4-AP) by 73 ± 10% ($n = 4$ slices, Fig. 1*E*) and thus most of the purine released under this condition is adenosine.

### 4-AP widens the presynaptic action potential

To understand how 4-AP increases purine release, we have investigated the actions of 4-AP on synaptic transmission at parallel fibre synapses, since parallel fibre (PF) activity is required for adenosine release in control (50–100 stimuli at 20 Hz in the absence of 4-AP, Wall & Dale, 2007). Application of 4-AP produced an increase in the amplitude of PF EPSPs (Fig. 2*A*). For example, at a concentration of 30 $\mu$M, 4-AP increased EPSP amplitude from 0.25 ± 0.05 mV to 1.2 ± 0.06 mV, $n = 4$. The increase in EPSP amplitude was accompanied by a reduction in the paired pulse ratio (50 ms interval, 60 $\mu$M 4-AP decreased the ratio from 1.32 ± 0.07 to 1.1 ± 0.06, $n = 4$, Fig. 2*B*) suggesting a presynaptic increase in glutamate release. A widening of the presynaptic parallel fibre volley (for example 30 $\mu$M 4-AP increased the volley half-width from 0.39 ± 0.1 ms to 0.47 ± 0.03 ms, $n = 4$, Fig. 2*C*) with no significant change in volley amplitude suggests the increase in glutamate release stems from enhanced release probability rather than the recruitment of extra parallel fibres.

### The properties of adenosine release resemble glutamate release from parallel fibres

Data from PF synapses demonstrate that 4-AP increases transmitter release by widening the presynaptic (parallel fibre) action potential. Since adenosine release in control (absence of 4-AP) is either from parallel fibres or parallel fibre activity is required for release (Wall & Dale, 2007), the amount of purines released in 4-AP should correlate with parallel fibre volley width. Increasing concentrations of 4-AP produced greater widening of the parallel fibre volley (Fig. 3*A*) and, as predicted, there was a close correlation ($r = 0.92$) between the width of the parallel fibre volley and the amount of purines released (Fig. 3*B*, filled circles).

### Enhanced adenosine release is partially mediated by glutamate receptor activation

In control conditions (absence of 4-AP), adenosine release is not affected by antagonists of ionotropic glutamate receptors (release evoked by 50–100 stimuli at 20 Hz, Wall

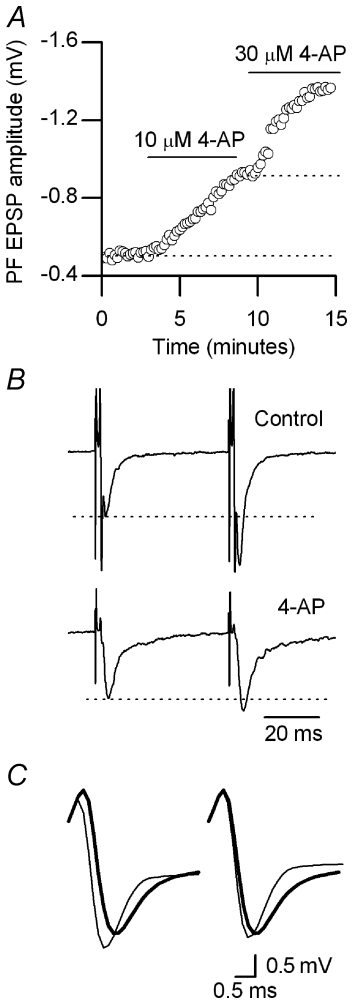


**Figure 2. 4-AP enhances parallel fibre glutamate release by widening the action potential**
*A*, graph plotting the amplitude of individual parallel fibre (PF) EPSPs against time. Application of 10 and then 30 $\mu$M 4-AP increased EPSP amplitude. *B*, superimposed averages of paired EPSPs (interval 50 ms) in control and in 30 $\mu$M 4-AP. The EPSPs were normalised to the amplitude of the first EPSP in control to illustrate the reduction in paired pulse facilitation produced by 4-AP. *C*, left panel, averages of the presynaptic volley (parallel fibre action potential) in control (thin line) and in 60 $\mu$M 4-AP (thick line). Right panel, the volleys superimposed showing the increase in volley duration produced by 4-AP with no increase in volley amplitude. Thus the increase in glutamate release stems from widening of the action potential rather than recruitment of additional parallel fibres.

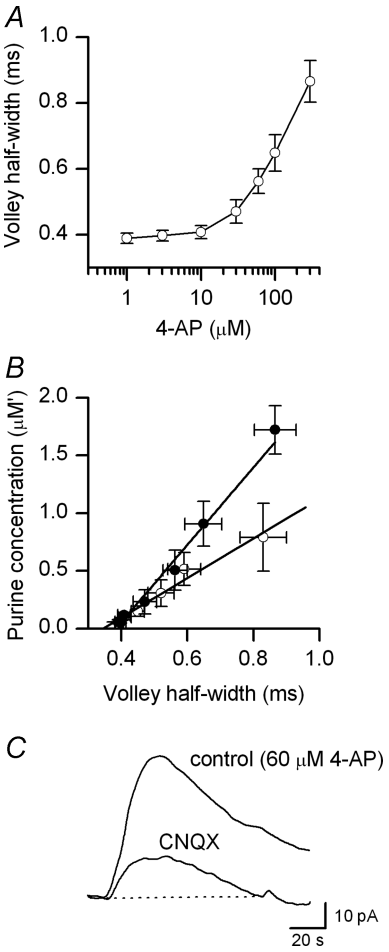


**Figure 3. Adenosine release grades with spike width**
*A*, parallel fibre-volley half-width plotted against 4-AP concentration ($n = 4$–6). *B*, the concentration of purines released plotted against volley half-width in control (filled circles) and in 20–50 $\mu$M CNQX (open circles). The linear fit in control (slope of 3.1, *R* value of 0.92) and CNQX (slope of 1.85, *R* value of 0.96) demonstrates that 40% of the signal is glutamate receptor dependent (all data from 40–100, 20 Hz stimuli, $n = 4$–6). *C*, superimposed traces from an adenosine (ADO) biosensor placed on the surface of the molecular layer in control (60 $\mu$M 4-AP) and in 4-AP plus CNQX (20 $\mu$M). Adenosine release (in response to fifty 20 Hz stimuli) was reduced by ~60% by CNQX.

& Dale, 2007). However, the greater amount of synaptically released glutamate in 4-AP could lead to the activation of additional cellular components which subsequently release purines. Application of the glutamate receptor antagonist CNQX (20 $\mu$M) reduced the ADO biosensor current (in 60 $\mu$M 4-AP) from 94 ± 19 pA to 37 ± 12 pA (~60% block, Fig. 3*C*, $n = 6$). Purine release was also reduced (by a similar amount) by other glutamate receptor antagonists: kynurenate (5 mM, $n = 3$) and NBQX (5 $\mu$M, $n = 3$). When glutamate receptors were blocked (CNQX 20–50 $\mu$M) there remained a strong correlation between parallel fibre volley width and the amount of purines released ($R = 0.96$, Fig. 3*B*, open circles) over a range of 4-AP concentrations with the slope of the relationship shallower than control (1.8 *vs.* 3.1, ~60% reduction) as expected. The close correlation of residual purine release with volley width in CNQX provides further evidence that glutamate receptor-independent extracellular purines arise from direct release from parallel fibres.

### No evidence that purine release results from extracellular ATP metabolism

Previous results suggest that released adenosine does not arise from extracellular ATP metabolism (Wall & Dale, 2007); however, due to the small amount of adenosine released and the low potency of nucleotidase inhibitors, it was not possible to completely exclude rapid breakdown of ATP before biosensor detection (Wall & Dale, 2007, 2008). We now take advantage of the significantly increased amounts of purines released in 4-AP to enhance the likelihood of biosensor detection of any putative upstream ATP. In 300 $\mu$M 4-AP, stimulation (40–100 stimuli, 20 Hz) resulted in a strong purine signal (1.8 ± 0.2 $\mu$M′, $n = 5$) with no measurable signal on the ATP biosensor (Fig. 4*A*). Even if the experiment was repeated in the presence of the most potent cerebellar nucleotidase inhibitor (Wall *et al.* 2008), POM-1 (100 $\mu$M), no ATP signal was revealed and the amount of purine detected was not significantly reduced (1.8 ± 0.2 *vs.* 1.6 ± 0.5 $\mu$M′, $n = 5$, Fig. 4*B*). To investigate the speed and extent of extracellular ATP metabolism, 10 $\mu$M ATP was injected into the slice (1 s pulse, see Methods). Large responses were produced on ATP biosensors (91 ± 23 pA equivalent to 1.1 ± 0.2 $\mu$M of ATP) with very little current on ADO biosensors (14 ± 7 pA equivalent to 65 ± 21 nM adenosine, $n = 5$, Fig. 4*C*). This provides strong evidence that ATP metabolism is insufficiently fast to prevent detection of putative upstream ATP during purine release and consequently that detected purines do not arise from extracellular ATP metabolism.

### Single-stimulus-induced adenosine release

The stimulation of adenosine release with single stimuli (in 60 $\mu$M 4-AP) has the advantage that the diffusive transport of adenosine within tissue can be examined from a source event that is highly localised in time, whereas in control (absence of 4-AP) the stimulation protocol to produce similar quantities of adenosine requires 2–5 s of continuous stimulation (Wall & Dale, 2007). The pharmacology of single-stimulus release is similar to the release from multiple stimuli in control (50–100 stimuli at 20 Hz, Wall & Dale, 2007): release is action potential dependent (blocked by 1 $\mu$M TTX, $n = 3$ slices) and $Ca^{2+}$ dependent (reversibly blocked by zero $Ca^{2+}$ aCSF, $n = 3$ slices), and the majority of the purine released is adenosine (~75%, Fig. 1*E*). However unlike control (absence of 4-AP) adenosine release, a large proportion of the adenosine released by a single stimulus

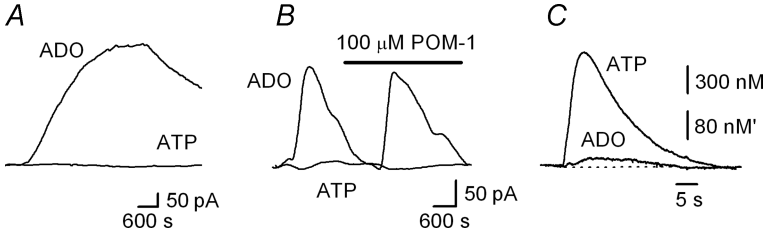


**Figure 4. No ATP detected despite enhanced purine release**
*A*, traces from an adenosine (ADO) biosensor placed on the surface of the molecular layer and an ATP biosensor placed within the same molecular layer in the presence of 300 $\mu$M 4-AP. Following stimulation (60 stimuli, 20 Hz), a significant purine concentration was detected by the ADO biosensor but there was no current on the ATP biosensor. *B*, traces from an adenosine (ADO) biosensor placed on the surface of the molecular layer and an ATP biosensor placed within the same molecular layer in the presence of 60 $\mu$M 4-AP. Blocking ectoATPAses with POM-1 (100 $\mu$M) did not reveal an ATP signal and did not reduce the ADO biosensor current. *C*, traces from an adenosine (ADO) biosensor and ATP biosensor placed within the molecular layer following a 1 s injection of 10 $\mu$M ATP. The ATP was injected at an equal distance (~1mm) from the ATP and ADO biosensors. The large ATP and small ADO biosensor currents demonstrate that the extracellular breakdown of ATP does not appear efficient enough to prevent biosensor detection of putative upstream ATP (top scale bar ATP, bottom scale bar ADO).

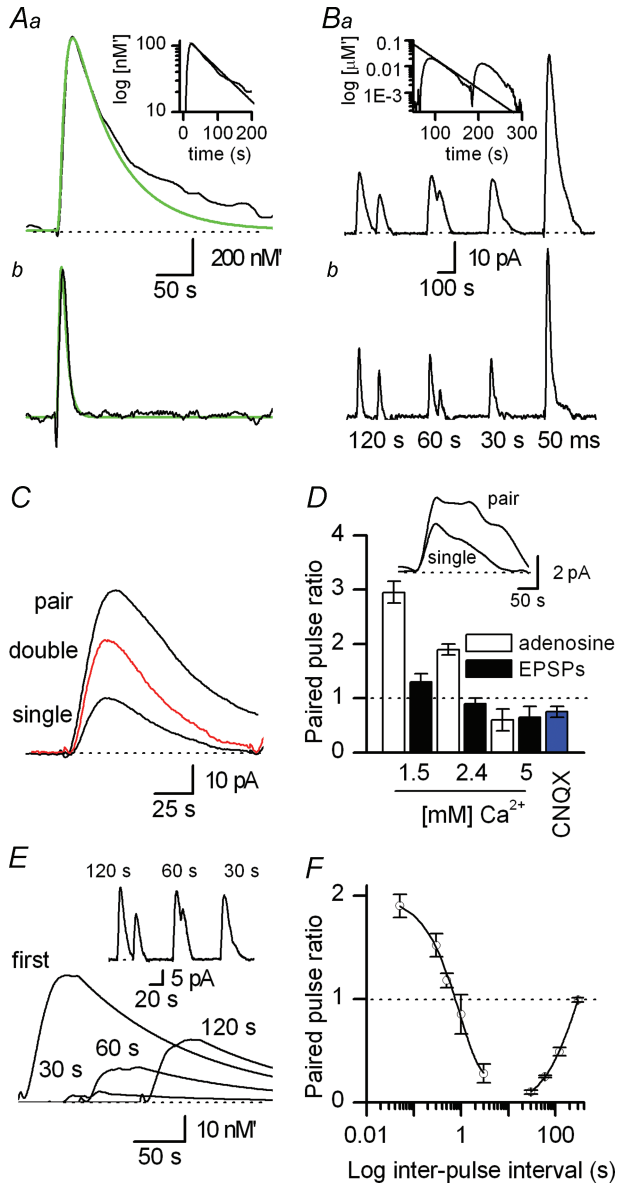


**Figure 5. Dynamics of single and paired stimulus-induced adenosine release**
*Aa*, ADO biosensor waveform in response to a single stimulus (black) compared to model (green). *Ab*, the deconvolved data (black) and model (green) from raw data in *Aa*. Inset shows exponential fit to data (time constant 60 s). *Ba*, ADO biosensor and *Bb* deconvolution waveforms (time constant 35 s) from a different experiment during paired-pulse stimulation protocols showing depression on minute time scales (interval 120 s, 60 s, 30 s) but strong facilitation at very short time scales (50 ms). *C*, ADO biosensor traces for a single stimulus and a pair of stimuli (interval 50 ms) highlighting the increased amplitude; the expected signal for twice the single-stimulus response is shown for comparison (red). *D*, effects of manipulation of extracellular $Ca^{2+}$ and glutamate receptor block (with CNQX in 2.4 mM $Ca^{2+}$) on the paired-pulse ratio for ADO biosensor amplitude and parallel fibre EPSP amplitude (for 50 ms intervals). Inset, ADO biosensor traces for a single stimulus and a 50 ms interval pair of stimuli recorded in 20 $\mu$M CNQX (2.4 mM $Ca^{2+}$). *E*, superimposed ADO biosensor traces (deconvolved and then reconvolved with baseline removed) for pairs of stimuli, inter-pulse intervals of 30 s, 60 s and 120 s, with an interval of 300 s between pairs. Increasing the inter-stimulus interval reduced the amount of depression. Inset, raw data used in *E*. *F*, graph plotting ADO biosensor paired-pulse amplitude ratio *versus* stimulation interval (log scale, $n = 4$–6). The decay in facilitation is fitted with a single exponential (time constant 0.9 s, *R* value 0.99) and the recovery from depression is fitted with a single exponential (time constant 280 s, *R* value 0.95). All traces in this figure were in 60 $\mu$M 4-AP.

is glutamate receptor dependent (20 $\mu$M CNQX reduced the current amplitude by $80 \pm 2\%$, $n = 5$). The selective AMPA receptor antagonist GYKI 47261 (10 $\mu$M) blocked $41 \pm 4\%$ ($n = 4$) of the biosensor current and thus a major proportion of the adenosine release stems from AMPA receptor activation.

### Diffusion model and deconvolution analysis

Single stimuli (300 s interval, 60 $\mu$M 4-AP) produced biosensor currents with a fast rise and slower exponential decay (Fig. 5*Aa*). The purine biosensor measures the combined concentration $P = A + I + H$ of adenosine ($A$), inosine ($I$) and hypoxanthine ($H$) in the neural tissue. The assumptions in this *minimal* diffusion model are: that the bulk (tissue-level) diffusion constant $D$ for each purine is similar; that the breakdown of hypoxanthine in tissue is slow compared to purine loss from the slice surface; and that the purines are released from the middle of the slice ($z = 0$) at a rate $F(t)$ uniformly per unit area of slice. If the variable $z$ measures the distance normal to the slice surface, then the combined purine concentration $P(t)$ obeys the following diffusion equation:

$$\frac{\partial P}{\partial t} = D\frac{\partial^2 P}{\partial z^2} + F(t)\delta(z).$$

The concentration at the two principal surfaces of the slice ($z = \pm h/2$) is assumed to be zero as it is open to the large volume of the bathing medium which is continuously washed out. Considering the example first of an impulse delivering a unit amount of purine per unit area at $t = 0$ so that $F(t) = \delta(t)$, the solution for the concentration $p(t)$ at a later time is:

$$p(t) = \frac{2}{h}\sum_{m=0}^{\infty} \exp\left(-t/\tau_m\right) \cos\left(\frac{z}{h}(2m+1)\pi\right)$$

where the time constants are a function of the slice thickness $h$:

$$\tau_m = \frac{h^2}{D(2m+1)^2\pi^2}.$$

Hence, the longest decay (zero mode $m = 0$) measured by the biosensor at the tail of the waveform is a function of the slice thickness and not purely a function of intrinsic tissue

parameters, like the diffusion constant or dependent on the properties of the biosensor (which have been omitted from this analysis). The biosensor is placed on a surface of the slice $z = h/2$ and measures the flux of purines leaving the slice $J(t)$. This flux is minus the gradient of the density multiplied by the diffusion constant $D$. Using the lower case $j(t)$ for the case of a unit impulse of purine per unit area injected at a time $t = 0$, we have:

$$j(t) = \frac{2D\pi}{h^2} \sum_{m=0}^{\infty} \exp(-t/\tau_m)(2m+1)(-1)^m.$$

This minimal theoretical waveform is compared to an experimental measurement in Fig. 5*Aa* and agrees well with initial rise and exponential fall. This implies that the response time of the biosensor is sufficiently fast to faithfully record the purine signal. If there are a series of purine pulses of concentration per unit area $c_k$ released at times $t_k$ then from the linearity of the diffusion equation the purine flux on the biosensor will be the sum:

$$J(t) = \sum_k c_k j(t - t_k).$$

A signature of the linearity will be that the decay of the waveform is (more-or-less) constant regardless of the amplitude (for example see Figs 5*B* and 6*C*).

A minimal diffusion model of adenosine transport in tissue predicts a biosensor current waveform $j(t)$ of the form:

$$j = \frac{2D\pi}{h^2} \sum_{m=0}^{\infty} e^{-\frac{t}{\tau_m}} (2m+1)(-1)^m \qquad (1)$$

where $D$ is the diffusion constant of purines within tissue and $h$ is the slice thickness. This formula resolves the biosensor current into a sum of modes of increasingly short time constants $\tau_m = \frac{h^2}{D(2m+1)^2\pi^2}$. For times greater than $h^2/D$ the only significant mode remaining is the zero order time constant $\tau_0 = \frac{h^2}{D\pi^2}$ – the slow decay seen on the biosensor. It can be noted that the model suggests this reflects loss of purines from the slice surface into the bathing medium. In Fig. 5*Aa* the time constant measured from an exponential fit (to the early component of the decay to avoid contamination from drift – see below) was 60 s. For a slice thickness of 400 $\mu$m this gives a

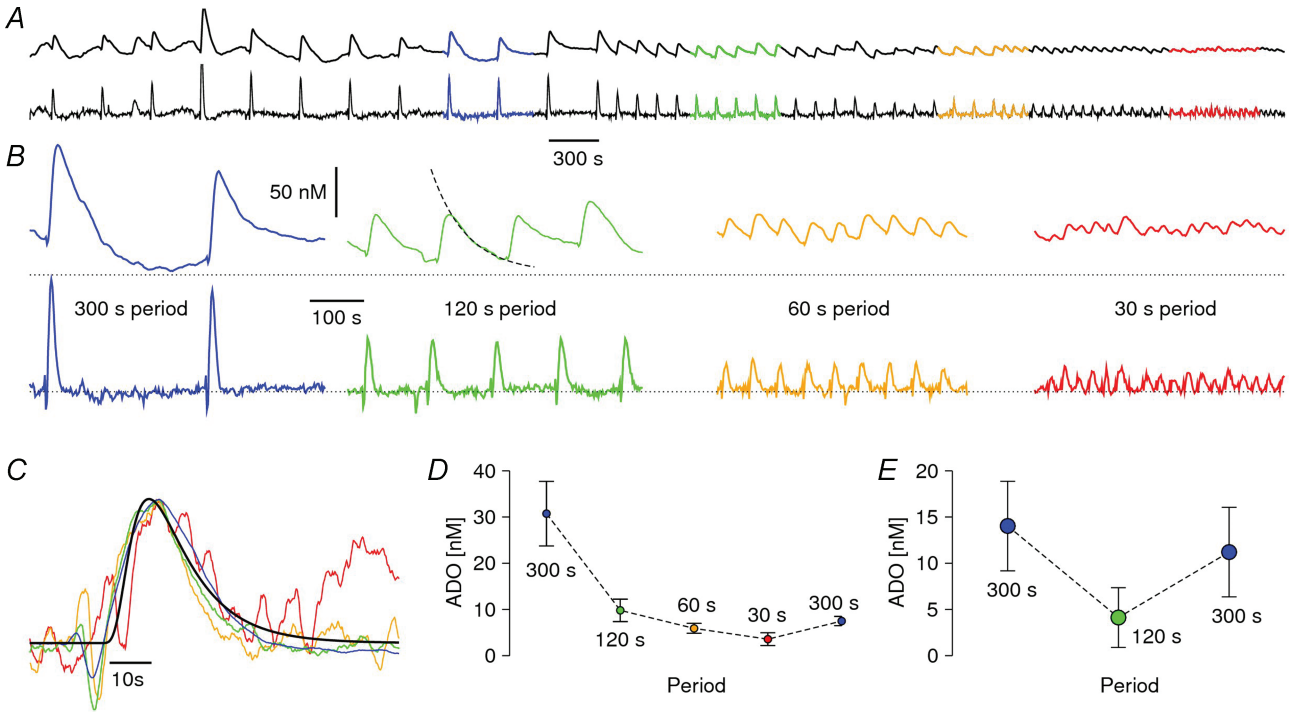


**Figure 6. Depression of adenosine release during repetitive single-pulse stimulation**
*A*, ADO biosensor trace (~2 h experiment) demonstrating stimulus interval-dependent levels of purine release with the deconvolutions (time constant 60 s) shown below. *B*, details for stimulus intervals of 300 s, 120 s, 60 s, 30 s (as marked) with deconvolutions shown below. An exponential fit (time constant 60 s) is shown in the in 120 s detail panel. The deconvolutions allowed for the amplitudes of overlapping adenosine waveforms to be accurately measured. *C*, detail of the deconvolved ADO traces for the intervals 300, 120, 60, 30 (same colour key) scaled to same amplitude showing waveform invariance. *D*, pooled data from multiple experiments including a return to 300 s stimulation to test recovery. There was an increase in amplitude during the 300 s period but it was small. *E*, recovery was greater for shorter duration experiments (stimulation period: three 300 s, four 120 s and three 300 s) in which a recovery of 80% was seen (panel shows amplitude mean and standard deviation).

model-dependent estimate of the diffusion constant of $D \approx 270\ \mu m^2\ s^{-1}$. Using these parameters extracted from the decay, the full waveform prediction can be compared to experiment and in Fig. 5*Aa* can be seen to be in good agreement capturing the initial rise and peak well.

This comparison with the initial component can be further examined by adapting a standard deconvolution method used in the analysis of intracellular recordings (Neher & Sakaba, 2001; Richardson & Silberberg, 2008). This procedure removes the slow exponential decay to reveal the fine details of the waveform. The linearity of the summed purine concentration allows for a simple deconvolution procedure to be applied to the signal. This procedure removes the long decay and leads to a trace of well separated deconvolved pulses. For cases where the original waveform tail is exponential, such as in the sum of post-synaptic potentials in intracellular voltage traces (Neher & Sakaba, 2001; Richardson & Silberberg, 2008) and the case of purine waveforms considered here, the deconvolution procedure is particularly simple and is achieved by differentiating the signal, multiplying it by the long time constant $\tau_0$ (which can be measured experimentally by fitting the purine waveform in a semi-log plot, see inset to Fig. 5*Aa*) and then adding it back to itself:

$$\mathrm{d}(t) = \tau_0 \frac{\mathrm{d}j}{\mathrm{d}t} + j,$$

see Fig. 5*Ab*. In terms of the model the deconvolved trace $\mathrm{d}(t)$ is:

$$\begin{aligned}\mathrm{d}(t) &= \tau_0 \frac{\mathrm{d}j}{\mathrm{d}t} + j \\ &= \frac{2D\pi}{h^2} \sum_{m=1}^{\infty} \exp(-t/\tau_m)(2m+1)(-1)^m \left(1 - \frac{\tau_0}{\tau_m}\right)\end{aligned}$$

in which it can be seen that the $m = 0$ mode is absent. Comparison of this with the data provides a finer test of the model (also plotted in Fig. 5*Ab*) and its assumptions.

The deconvolution procedure is particularly useful for measuring the amplitude of overlapping waveforms, for example see Figs 5*B* and 6*A* and *B*. The method is to deconvolve the waveform and then crop out the deconvolved pulses and reconvolve (reverse the deconvolution process) using the formula:

$$A(t) = \int_{-\infty}^{t} \frac{\mathrm{d}t'}{\tau_0}\, \mathrm{d}(t') \exp(-(t - t')/\tau_0).$$

This yields separated ADO waveforms from which the amplitudes can be directly measured, Figs 5*B* and *E* and 6*B*. Further details of the methodology (applied to intracellular voltage traces) can be found in Richardson & Silberberg (2008). Even at this higher level of detail the agreement between model and experiment is close. Given that the model is predicated on an instantaneous impulse of adenosine into the tissue, this close match between theory and experiment suggests the single-stimulus release event is highly localised in time with a subsecond duration.

### Plasticity of the waveform amplitude

To investigate the dynamics of the quantity of adenosine released under multiple single-stimulus events we first used a paired-pulse protocol. Inter-pulse intervals between 50 ms and 120 s were used with a 300 s interval between pairs. However, because the adenosine waveform has a slow decay (in the range of 50–150 s, but constant for a particular slice) the second waveform is often superimposed on the tail of the preceding one, complicating accurate amplitude measurement. In analogy with the treatment of intracellular recordings (Neher & Sakaba, 2001; Richardson & Silberberg, 2008) we applied the deconvolution method (outlined above) to resolve the pulses and allow for accurate amplitude measurement of overlapping waveforms (see Figs 5*B* and 6*B*). The plasticity of adenosine release was complex exhibiting both facilitation and depression, depending on the stimulus interval.

**Facilitation over millisecond time scales.** At short intervals marked facilitation occurred, with significantly more adenosine released from the second stimulus compared to the first (50 ms interval, paired-pulse ratio $1.9 \pm 0.1$, $n = 8$, Fig. 5*C* and *D*). To investigate the facilitation mechanism, extracellular $Ca^{2+}$ concentrations were varied. Facilitation at 50 ms intervals was significantly ($P < 0.05$) increased in low $Ca^{2+}$ (1.5 mM, paired pulse ratio $3 \pm 0.2$, $n = 4$, Fig. 5*D*) and significantly ($P < 0.05$) decreased in high $Ca^{2+}$ (5 mM, paired-pulse $0.6 \pm 0.1$, $n = 4$, Fig. 5*D*). The paired pulse plasticity of parallel fibre EPSPs (and therefore glutamate release) was also $Ca^{2+}$ dependent (Fig. 5*D*). To investigate whether glutamate receptor activation is required for the facilitation of adenosine release at short intervals, glutamate receptors were blocked (with 20 $\mu$M CNQX). CNQX abolished the facilitation of adenosine release (paired pulse ratio $0.75 \pm 0.1$, $n = 6$, Fig. 5*D*, inset) suggesting that the facilitation does require glutamate receptor activation.

**Depression over minute time scales.** As the inter-pulse interval was increased, the degree of facilitation decreased to be replaced by depression. At 30 s intervals the second pulse was almost absent and was seen to recover gradually for stimulations at 60 s and 120 s intervals (Fig. 5*E*). These dynamics can be captured by adapting a resource-depletion model used to model synaptic

depression in the context of fast neurotransmitter vesicle release (Tsodyks & Markram, 1997) of the form:

$$\frac{dS}{dt} = \frac{S_0 - S}{\tau_s} + fS\sum\delta(t - t_k) \quad (2)$$

where $S(t)$ is the current level of releasable purine stores, $S_0$ is the maximum level of the store, $\tau_S$ is the restock time constant and $f$ is the fraction of the store (evaluated just before the release event) released on each stimulation times $t_k$. Hence on the arrival of a stimulus the quantity of purine released is $fS(t)$. From Fig. 5*E* it is inferred that the fraction $f$ of stores released is very close to 1 (under single stimulation in 60 $\mu$M 4-AP, see Discussion) so that on stimulation the entire current store $S(t)$ is released, depleting the store to zero. This predicts an exponential recovery from full depletion so that the releasable stores follow the equation:

$$S(t) = S_0\left(1 - e^{-\frac{t}{\tau_S}}\right).$$

**Summary of paired-pulse plasticity.** The interval-dependent plasticity is summarised in Fig. 5*F*. Facilitation decreased exponentially with increasing intervals of stimulation with a time constant of 1.0 s. Depression recovered exponentially with increasing intervals of stimulation with a time constant of 280 s, which can be identified with the parameter $\tau_S$ of the depletion–restock model. The presence of facilitation and depression within the same stimulated pathway suggests that facilitation involves the recruitment of an additional adenosine source, presumably via increased glutamate receptor activation.

### Depression and recovery during continued stimulation

Cerebellar networks receive on-going activation *in vivo* and so to further investigate depression and recovery over minute time scales we examined the amplitude dynamics under continuous stimulation with periods in the range of 30–300 s (Fig. 6*A*, $n = 5$ slices). Period-dependent amplitudes were seen with shorter periods leading to ADO waveforms of lower amplitude, as expected from the paired-pulse protocol and store depletion–restock model. Note that the mean offset from baseline for 60 s and 30 s stimulation are similar due to the amplitudes halving as the period doubles. This is predicted from the resource-depletion model for stimulations periods shorter that the restock time constant for which the released stores are expected to follow the formula $S(T) \approx S_0 T/\tau_S$ where $T$ is the stimulation period. The implication is that at high stimulation rate the net amount of adenosine released per unit time $S(T)/T = S_0/\tau_S$ becomes independent of stimulation frequency $1/T$ and is limited by the maximum store level and the restock rate $1/\tau_S$; this is a feature also seen in vesicle-release dynamics of fast neurotransmitters (Tsodyks & Markram, 1997).

The fine details of the waveforms are also shown in Fig. 6*A* and *B* through deconvolution of the ADO biosensor traces. The deconvolved waveforms for different stimulation periods are shown to be invariant to the period of stimulation in Fig. 6*C* showing constancy of the underlying release process with a change only in its degree. In Fig. 6*D* mean ADO biosensor waveform amplitudes are plotted as a function of stimulation interval, with a period of 300 s intervals performed at the end of the experiment to measure the degree of recovery. The amplitude doubled from the 30 s period epoch to the 300 s period epoch but regained only 25% of its initial amplitude when compared to the earlier 300 s period epoch. This partial recovery is not consistent with the paired pulse data, in which full recovery was consistently seen after ~300 s. Reasons for the discrepancy could be an additional depression or depletion mechanism acting over a longer time scale than $\tau_S$ or, given the duration of the experiments (2 h) and number of intervening purine-releasing stimuli (>50), a degradation of the purine production in the slice. The latter reason is consistent with additional experiments of shorter duration and stimulation number (three 300 s, five 120 s, three 300 s concurrent periods) in which the recovery was 81 ± 3% ($n = 4$, Fig. 6*E*).

## Discussion

In agreement with many studies (Nedergaard, 1999; Daniel & Crepel, 2001; Mitterdorfer & Bean, 2002), the partial block of presynaptic $K^+$ channels prolongs action potential duration leading to an increase in $Ca^{2+}$ influx and neuronal transmitter release. At parallel fibre synapses, EPSCs are very sensitive to spike broadening; a 23% increase in spike width leads to a 25% increase in total calcium influx, which doubles synaptic strength (Sabatini & Regher, 1997). The strong correlation between parallel fibre action potential duration and the amount of purines released further supports the involvement of parallel fibres in purine release. We believe that this is the first demonstration that purine release, like that of conventional neurotransmitters, depends upon action potential width.

Our use of 4-AP as a tool to enhance adenosine release has enabled us to study the release in much greater detail in response to a single spike (more reproducible and better defined temporally) as opposed to trains of spikes, which will exhibit more variability and are less amenable to analysis and experimental manipulation. Nevertheless we expect that the mechanisms we have uncovered by using 4-AP to enhance release also pertain to adenosine release

under more physiological conditions in the absence of 4-AP.

### A significant component of the adenosine release is glutamate receptor dependent

The glutamate receptor-mediated component of purine release, revealed in 4-AP, may arise because the increased release of glutamate activates additional cellular components. The glutamate could feed back to enhance release via presynaptic glutamate receptors, for example via facilitatory kainate autoreceptors that are present on parallel fibre terminals (Delaney & Jahr, 2002). Or the glutamate could activate a peri/postsynaptic cellular component leading to purine release. AMPA/kainate receptors are present on Bergmann glial cells (Clark & Barbour, 1997; Bordey & Sontheimer, 2003; Bellamy & Ogden, 2006) and there is evidence that glial cells can release adenosine, although this is in response to hypoxia/ischaemia (Martin *et al*. 2007). AMPA receptors are also present on the axons of molecular layer interneurones, which have been suggested to release ATP (Piet & Jahr, 2007; Rossi *et al*. 2008). This seems an unlikely source of the detected purines as we have been unable to detect any ATP (see below).

### Evidence is against adenosine arising from extracellular ATP metabolism

Even with increased purine release, it was not possible to measure any extracellular ATP release. The limit of ATP detection is ∼60 nM producing 10 pA of current on the ATP biosensor (Wall & Dale, 2007). In the presence of 300 $\mu$M 4-AP, ∼1.8 $\mu$M of purines was detected and thus to be below the limits of detection more than 96% of the ATP has to be broken down before reaching the ATP biosensor. The injection of pulses of ATP into cerebellar slices and its subsequent measurement on ATP biosensors suggests that ATP metabolism is not efficient enough to remove ATP before detection. Application of POM-1, a potent ecto-ATPase inhibitor (blocking ∼60% of ATP breakdown, Wall *et al.* 2008) did not reveal ATP release and did not reduce the purine signal. Thus we are unable to provide any evidence that the action potential-dependent release of purines arises from extracellular ATP metabolism.

Increases in Bergmann glia intracellular $Ca^{2+}$ concentration following parallel fibre stimulation can be blocked by pyridoxal phosphate 6-azophenyl-2′,4′-disulfonic acid (PPADS) suggesting the release of ATP (Beierlein & Regehr, 2006; Piet & Jahr, 2007). The source of this ATP could be molecular layer interneurones (Piet & Jahr, 2007). Although our stimulus will activate molecular layer interneurones (directly or via AMPA receptors), we were unable to detect any ATP. Thus the amount of ATP released must be either very small or highly localised and is therefore unlikely to account for the large adenosine signals we observe.

### Plasticity of adenosine release in response to single stimuli

In the presence of 4-AP it was possible to release adenosine in response to a single stimulus (equivalent to a single action potential, but see Isope *et al*. 2004), which has allowed us to investigate adenosine release with unprecedented detail. The resulting waveforms of adenosine release were highly reproducible and featured a fast rise followed by an exponential decay. The waveform was accurately described by a minimal diffusion model that accounted for loss of purines via the slice surface. The close agreement with the rise of the waveform suggests that the adenosine release is a sharp event, taking place over a subsecond time scale.

Paired stimuli illustrated a rich history-dependent dynamics for the amplitude of released adenosine. Both facilitation and depression were seen depending on the inter-pulse interval. Facilitation of adenosine release occurred at short inter-pulse intervals (less than 500 ms) and was dependent on extracellular $Ca^{2+}$ concentration as might be expected for conventional exocytosis of neurotransmitter. However, this facilitation was abolished by blocking glutamate receptors. One hypothesis that could possibly explain the data is that incomplete clearance of the glutamate released by the first stimulus coupled with additional glutamate release from the second stimulus leads to greater glutamate overspill and activation of previously naive cellular components. There is evidence for the overspill of parallel fibre glutamate, provided by experiments investigating the activation of Purkinje cell metabotropic glutamate receptors (mGluRs). The firing of one or two action potentials does not activate perisynaptic mGluRs, but firing five action potentials (at 100 Hz) releases enough glutamate to activate mGluRs (Brasnjo & Otis, 2001). Thus if enough glutamate is released it cannot be cleared before entry into the perisynaptic space. Components that could be activated by glutamate include presynaptic parallel fibres (Delaney & Jahr, 2002), perisynaptic Bergmann glia (Clark & Barbour, 1997; Bordey & Sontheimer, 2003; Bellamy & Ogden, 2006) or postsynaptic interneurones (Rossi *et al*. 2008). From the current data it is not possible to distinguish between these potential additional sources of adenosine.

With longer inter-pulse intervals (30–120 s), depression of adenosine release dominated. Using trains of stimuli, we found that the amount of adenosine released per unit time remained constant, which is characteristic of a simple depletion and refill model. The constancy of the underlying waveform, studied in fine detail using deconvolution analysis, suggests that depression results

simply from a reduction in the amount of adenosine released rather than changes in the actual release process. There could be true depletion of adenosine stores, as demonstrated following hypoxia (Pearson *et al*. 2001) and in the hypothalamic defence reflex (Dale *et al*. 2002), or a functional depletion as a result of reduced glutamate receptor activation. We have little evidence for the latter but the probable saturation of glutamate receptors in the synaptic cleft means it is not possible to completely exclude it.

### Adenosine dynamics in control conditions

In this study the amplification of the adenosine release process using 4-AP was used to produce waveforms from which the adenosine transport in tissue and history dependence of the quantity released could be reliably measured. Because the diffusion and transport is additively linear, even at high concentrations (this is seen in the long decay being constant regardless of waveform amplitude), it can be expected that the stock depletion–restock model in eqn (2) holds for adenosine release due to stimulation in concentrations of 4-AP that are less than 60 $\mu$M. The history dependence, however, will be different. Consideration of eqn (2) and the number of stimuli required to produce a constant, measureable signal in various concentrations of 4-AP (Fig. 1*C*) suggests that in control eqn (2) would still hold, but with the fraction $f$ of adenosine released from stores of the order of 0.5–2% per stimulus, rather than the 100% in 60 $\mu$M 4-AP. Given that the restock time constant is of the order of hundreds of seconds and that *in vivo* parallel fibre activation will be of relatively high rate, the model predicts that the adenosine release will nevertheless be in the depleted restock-rate-limited regime, despite the smaller fraction of release.

This is the first time that adenosine release and transport have been examined in such fine quantitative detail. We have demonstrated that adenosine release can have a rich and complex dynamics, sharing many properties of the better studied neurotransmitters including rapid release, dependence on spike width, reproducible waveforms, and history-dependent amplitudes showing both facilitation and depression.

## References


Beierlein M & Regehr WG (2006). Brief bursts of parallel fiber activity trigger calcium signals in Bergmann glia. *J Neurosci* **26**, 6958–6967.

Bellamy TC & Ogden D (2006). Long-term depression of neuron to glial signalling in rat cerebellar cortex. *Eur J Neurosci* **23**, 581–586.

Bordey A & Sontheimer H (2003). Modulation of glutamatergic transmission by Bergmann glial cells in rat cerebellum *in situ*. *J Neurophysiol* **89**, 979–988.

Boison D (2006). Adenosine kinase, epilepsy and stroke, mechanisms and therapies. *Trends Pharmacol Sci* **27**, 652–658.

Brasnjo G & Otis TS (2001) Neuronal glutamate transporters control activation of postsynaptic metabotropic glutamate receptors and influence cerebellar long-term depression. *Neuron* **31**, 607–616.

Clark BA & Barbour B (1997). Currents evoked in Bergmann glial cells by parallel fibre stimulation in rat cerebellar slices. *J Physiol* **502**, 335–350.

Craig CG & White TD (1993). N-Methyl-D-aspartate and non-N-methyl-D-aspartate-evoked adenosine release from rat cortical slices, distinct purinergic sources and mechanisms of release. *J Neurochem* **60**, 1073–1080.

Dale N (1998). Delayed production of adenosine underlies temporal modulation of swimming in frog embryo. *J Physiol* **511**, 265–272.

Dale N, Gourine AV, Llaudet E, Bulmer D, Thomas T & Spyer KM (2002). Rapid adenosine release in the nucleus tractus solitarii during defence response in rats, real-time measurement *in vivo*. *J Physiol* **544**, 149–160.

Dale N & Frenguelli B (2009). Release of adenosine and ATP during ischemia and epilepsy. *Curr Neuropharmacol* **7**, 160–179.

Daniel H & Crepel F (2001). Control of $Ca^{2+}$ influx by cannabinoid and metabotropic glutamate receptors in rat cerebellar cortex requires $K^+$ channels. *J Physiol* **537**, 793–800.

Delaney AJ & Jahr CE (2002). Kainate receptors differentially regulate release at two parallel fiber synapses. *Neuron* **36**, 475–482.

Edwards FA, Gibb AJ & Colquhoun D (1992). ATP receptor-mediated synaptic currents in the central nervous system. *Nature* **359**, 144–147.

Fredholm BB, Arslan G, Halldner L, Kull B, Shulte G & Wassweman W (2000). Structure and function of adenosine receptors and their genes. *Naunyn Schmiedebergs Arch Pharmacol* **362**, 364–374.

Fredholm BB, Ijzerman AP, Jacobson KA, Klotz KN & Linden J (2001). International Union of Pharmacology. XXV. Nomenclature and classification of adenosine receptors. *Pharmacol Rev* **53**, 527–552.

Isope P, Franconville R, Barbour B & Ascher P (2004). Repetitive firing of rat cerebellar parallel fibres after a single stimulation. *J Physiol* **554**, 829–839.

Jo YH & Schlichter R (1999). Synaptic co-release of ATP and GABA in cultured spinal neurons. *Nat Neurosci* **2**, 241–245.

Kimura M, Saitoh N & Takahashi T (2003). Adenosine A1 receptor-mediated presynaptic inhibition at the calyx of Held of immature rats. *J Physiol* **553**, 415–426.

Li J & Iadecola C (1994). Nitric oxide and adenosine mediate vasodilation during functional activation in cerebellar cortex. *Neuropharmacol* **33**, 1453–1461.

Llaudet E, Botting N, Crayston J & Dale N (2003). A three enzyme microelectrode sensor for detecting purine release from central nervous system. *Biosens Bioelectron* **18**, 43–52.

Llaudet E, Hatz S, Droniou M & Dale N (2005). Microelectrode biosensor for real-time measurement of ATP in biological tissue. *Anal Chem* **77**, 3267–3273.

Martín ED, Fernández M, Perea G, Pascual O, Haydon PG, Araque A & Ceña V (2007). Adenosine released by astrocytes contributes to hypoxia-induced modulation of synaptic transmission. *Glia* **55**, 36–45.

Mitchell JB, Lupica CR & Dunwiddie TV (1993). Activity-dependent release of endogenous adenosine modulates synaptic responses in the rat hippocampus. *J Neurosci* **13**, 3439–3447.

Mitterdorfer J & Bean BP (2002). Potassium currents during the action potential of hippocampal CA3 neurons. *J Neurosci* **22**, 10106–10115.

Nedergaard S ( 1999). Regulation of action potential size and excitability in substantia nigra compacta neurons, sensitivity to 4-aminopyridine. *J Neurophysiol* **82**, 2903–2913.

Neher E & Sakaba T (2001). Combining deconvolution and noise analysis for the estimation of transmitter release rates at the calyx of Held. *J Neurosci* **21**, 444–461.

Pearson RA, Dale N, Llaudet E & Mobbs P (2005). ATP released via gap junction hemichannels from the pigment epithelium regulates neural retinal progenitor proliferation. *Neuron* **46**, 731–744.

Pearson T, Nuritova F, Caldwell D, Dale N & Frenguelli BG (2001). A depletable pool of adenosine in area CA1 of the rat hippocampus. *J Neurosci* **21**, 2298–2307.

Piet R & Jahr CE (2007). Glutamatergic and purinergic receptor-mediated calcium transients in Bergmann glial cells. *J Neurosci* **27**, 4027–4035.

Richardson MJE & Silberberg G (2008). Measurement and analysis of postsynaptic potentials using a novel voltage-deconvolution method. *J Neurophysiol* **99**, 1020–1031.

Rossi B, Maton G & Collin T (2008). Calcium-permeable presynaptic AMPA receptors in cerebellar molecular layer interneurones. *J Physiol* **586**, 5129–5145.

Sabatini BL & Regehr WG (1997). Control of neurotransmitter release by presynaptic waveform at the granule cell to Purkinje cell synapse. *J Neurosci* **17**, 3425–3435.

Sweeney MI ( 1996). Adenosine release and uptake in cerebellar granule neurons both occur via an equilibrative nucleoside carrier that is modulated by G proteins. *J Neurochem* **67**, 81–88.

Tsodyks M & Markram H (1997). The neural code between neocortical pyramidal neurons depends on neurotransmitter release probability. *Proc Natl Acad Sci U S A* **94**, 719–723.

Wall MJ & Dale N (2007). Auto-inhibition of parallel fibre–Purkinje cell synapses by activity dependent adenosine release. *J Physiol* **581**, 553–566.

Wall MJ & Dale N (2008). Activity-dependent release of adenosine: a critical re-evaluation of mechanism. *Curr Neuropharmacol* **6**, 329–337.

Wall MJ, Wigmore G, Lopatár J, Frenguelli BG & Dale N (2008). The novel NTPDase inhibitor sodium polyoxotungstate (POM-1) inhibits ATP breakdown but also blocks central synaptic transmission, an action independent of NTPDase inhibition. *Neuropharmacol* **55**, 1251–1258.

Wong YC, Billups B, Johnston J, Evans RJ & Forsythe ID (2006). Endogenous activation of adenosine A1 receptors but not P2X receptors during high-frequency synaptic transmission at the calyx of Held. *J Neurophysiol* **95**, 3336–3342.

## Author contributions

The experiments were performed in the laboratory of M.J.W. Original concept for research: M.J.W. and N.D. The research was designed by B.P.K., M.J.E.R., N.D. and M.J.W. Data were collected by B.P.K. and analysed by B.P.K. and M.J.E.R. Mathematical models were developed by M.J.E.R. The manuscript was written by M.J.W. and M.J.E.R. with assistance from B.P.K. and N.D. All authors have read and approved the final version of the manuscript.

## Acknowledgements

This work was supported by the Medical Research Council UK (MRC). M.J.E.R. acknowledges support from the Research Councils United Kingdom (RCUK).